Contrails

FINITE ELEMENT STIFFNESS MATRICES FOR ANALYSIS OF PLATE BENDING

Ray W. Clough*
University of California, Berkeley, California

and

James L. Tocher**
The Boeing Company, Renton, Washington

A study is made of the relative accuracy provided by seven different types of finite elements in the approximate analysis of plate bending. The Kirchoff plate bending theory is assumed, and stiffness matrices for three rectangular and four triangular elements are considered. Included among these is a newly developed triangular element which provides for full displacement compatibility along the edges of adjacent elements. Analyses are made with each of these elements of the central deflection in eight different rectangular plate systems, using five different mesh sizes. Two of the rectangular elements and the compatible triangular element are found to give results which converge toward the correct answer as the mesh size is refined.

1.0 INTRODUCTION

The finite element method provides a convenient and powerful technique for the analysis of problems of continuum mechanics. Since its original development during the early 1950's, the method has been applied to a wide variety of problems with noteworthy success. One of the greatest virtues of the method is its versatility: the same general technique is employed in analyzing the stresses and deflections in any type of elastic continuum, and both loading conditions and boundary conditions may be completely arbitrary.

The general features of the finite element analysis procedure are well known and need not be presented here in detail. Previous applications range from problems of plane stress (References 1 and 2) and axially symmetric solids (Reference 3) to the analysis of plates (Reference 4) and shells (References 5 and 6). In addition to treatment of these two-dimensional systems, more limited investigations have been made with the analysis of general three-dimensional solids by this technique. (References 7 and 8)

The essential feature of the finite element method is the means by which the differential equations of equilibrium of the elastic continuum are approximated by a set of algebraic equilibrium equations. This procedure is generally looked upon as the substitution for the actual continuum of an assemblage of discrete structural elements, interconnected at a finite number of nodal points. In effect, the continuum may be visualized as being physically cut up into the finite element system, the material properties of the original material being retained in the elements. The analysis involves the evaluation of the element elastic properties, which are represented by the stiffness matrix expressing the relationship between element nodal forces and displacements. By appropriate superposition of these element stiffnesses, the stiffness matrix of the entire assemblage may be obtained. Finally, the nodal force equilibrium

*Professor of Civil Engineering
**Research Specialist, Airplane Division

Approved for Public Release

Contrails

equations, expressed in terms of this structural stiffness matrix, must be solved simultaneously for the nodal displacements of the complete system.

This same sequence of operations may be used to analyze any elastic continuum. The critical steps, which control the accuracy of the approximation, are the physical idealization or subdivision into the finite element system, and the manner in which the element stiffnesses are evaluated. The most general method for defining the element stiffnesses is based upon assuming that the deformations within each element are limited to a restricted set of patterns or generalized coordinates, and the accuracy of the solution is directly dependent upon the extent to which these assumed deformations can approximate the true distortions of the continuum.

It is of interest to note that the assumption of the displacement patterns for the various discrete element zones of the continuum is a special form of the Rayleigh-Ritz procedure (Reference 9). Therefore it is not necessary to visualize the physical separation of the continuum into discrete elements; instead one may simply introduce assumed displacement functions for selected zones of the continuum and look upon the analysis as a Rayleigh-Ritz process. There are definite advantages, however, in retaining the physically discrete element concept when analyzing complex systems involving the interconnection of two or more different types of elements.

The purpose of this paper is to present further developments in the application of the finite element method to the analysis of plate bending. Comparisons are made of the accuracy of results obtained with various stiffness matrices which have been employed previously for both rectangular and triangular finite elements. In addition, a new, fully compatible, triangular element is introduced and shown to be significantly better than any triangular plate bending element previously described in the literature. In each of the elements considered, the convergence qualities of the idealization are evaluated as the mesh size is successively refined.

ANALYSIS OF ELEMENT STIFFNESS

Displacement Pattern Requirements

It is evident that the accuracy which may be obtained by the finite element method depends directly on the extent to which the assumed deformation patterns are able to reproduce the distortions actually developed within the continuum. In general, the finer the finite element mesh, the more realistic will be the results; but the deformations will not necessarily converge to the correct values even with an infinitesimal mesh size unless the deformation patterns within the element are properly chosen. On the other hand, very good results may be obtained with a very coarse mesh if the element deformation patterns are of an appropriate type. Thus, the most critical factor in the entire finite element analysis is the selection of the element deformation functions.

Basic guides to the selection of suitable element deformation functions have been set forth previously (Reference 10); they may be summarized as follows:

(1) All possible rigid body displacements must be included; otherwise the conditions of statics will be grossly violated.

(2) All uniform strain states should be included; otherwise the finite element idealization cannot represent the true state of strain no matter how fine the mesh is made.

Approved for Public Release

Contrails

(3) Conditions of compatibility should be satisfied along the boundaries between elements as well as within the elements.

If all of these conditions are met, the finite element idealization will provide a lower bound to the strain energy of the system, and the results will converge toward the true state of deformation as the mesh size is reduced.

Element Analysis Procedure

Methods of calculating element stiffness matrices have been discussed previously (Reference 11) and need not be presented here in detail. However, the procedure used in this investigation will be outlined for the sake of completeness. The basic steps involved are as follows; (wherein all symbols represent matrices):

(1) Express element displacements in terms of assumed displacement patterns having amplitudes α:

$$\mathbf{r} = \mathbf{M}\alpha \tag{1}$$

The displacement functions, **M**, should satisfy the requirements listed above, and should be equal in number to the degree of nodal point freedom of the element. A greater number of displacement functions may be assumed and reduced to the required number of degrees of freedom by a Rayleigh-Ritz procedure (References 12 and 13), but this refinement does not appear to be worth while in most cases.

(2) Compute element strains, ϵ:

$$\epsilon = \mathbf{B}\alpha \tag{2}$$

where the matrix B is obtained by appropriate differentiation of **M**.

(3) Compute element stresses, σ:

$$\sigma = \mathbf{D}\,\mathbf{B}\,\alpha \tag{3}$$

in which D represents the material stress-strain relationships.

(4) Compute the generalized coordinate element stiffness, $\bar{k}$:

$$\bar{\mathbf{k}} = \int \mathbf{B}^T \mathbf{D}\,\mathbf{B}\; dV \tag{4}$$

(5) Compute nodal displacements, r_i:

$$\mathbf{r}_i = \mathbf{A}\,\alpha \tag{5}$$

where **A** is obtained by introducing the nodal coordinates into the displacement functions, **M**.

(6) Transform to the element stiffness **k** expressed in terms of nodal coordinates

$$\mathbf{k} = \left(\mathbf{A}^{-1}\right)^T \bar{\mathbf{k}} \left(\mathbf{A}^{-1}\right) \tag{6}$$

Approved for Public Release

Contrails

PLATE BENDING ELEMENT STIFFNESSES

All the plate bending stiffnesses considered in this study were evaluated by the above described procedure. The Kirchhoff plate bending theory was assumed to be applicable, so the deformations of the plate elements are completely defined by the lateral displacement w (x,y) . . On this basis, the plate elements are seen to have three degrees of freedom per nodal point: the normal displacement and two rotation components. Thus a triangular plate element has 9 degrees of freedom, while a rectangular plate has 12. The types of deformation assumptions on which each of the element stiffness analyses was based will be described briefly; code letters will be assigned to distinguish the various cases. The coefficients of the rectangular element stiffness matrices are listed in the Appendix; explicit expressions were not derived for the coefficients of the triangular element stiffness matrices.

Rectangular Elements

1. (ACM) The simplest expression which has been used in defining the rectangular element stiffness is the 12-term polynomial in x and y:

$$w = \alpha_1 + \alpha_2 x + \alpha_3 y + \alpha_4 x^2 + \alpha_5 xy + \alpha_6 y^2 + \alpha_7 x^3 + \alpha_8 x^2 y + \alpha_9 x y^2 + \alpha_{10} y^3 + \alpha_{11} x^3 y + \alpha_{12} x y^3 \tag{7}$$

The two fourth-degree terms which were included to provide the required number of displacement patterns were selected to maintain symmetry and also to satisfy the biharmonic equilibrium equation. This expression was used by Adini and Clough (Reference 14) and gives results which are identical to those resulting from a different form of expression proposed by Melosh (Reference 15).

2. (M) In an earlier paper (Reference 16), Melosh proposed a different plate bending stiffness matrix, which was developed on the basis of physical reasoning. In resisting bending, the plate is assumed to distort along the edges with shapes defined by beam displacement functions. These displacements are assumed to decrease linearly toward the opposite edge. In addition, it is assumed that twisting effects are resisted by a state of uniform twist in the element, which distorts the element to a simple hyperbolic-paraboloid shape.

3. (P) The displacement functions described in the two preceding cases do not satisfy completely the compatibility requirements along the edges of the rectangular elements. Vertical displacement compatibility is achieved, but the normal slopes may be different at the edges of adjacent elements. A set of displacement functions which completely satisfy compatibility requirements may be obtained by considering separately the nodal displacements applied at each corner. These functions were first employed by Papenfuss (Reference 17); they were developed independently by the authors of this paper before this reference was brought to their attention.

Consider joint "i" of the rectangular element shown in Figure 1 if a unit vertical displacement is applied at this joint, the displacements of the plate may be approximated by the expression:

$$w_i = \psi(\xi)\,\psi(\eta) \tag{8}$$

where ψ represents the nondimensionalized displacement function of a uniform beam subjected to a unit translation at one end without rotation, as shown in the figure. Similarly, if

Approved for Public Release

Contrails

a unit rotation in the x direction is applied at joint "i", the plate displacements may be approximated by the expression:

$$w_2 = \phi(\xi)\psi(\eta) \tag{9}$$

whereas if a unit rotation is applied in the y direction, the approximate shape is given by:

$$w_3 = \psi(\xi)\phi(\eta) \tag{10}$$

In both of these expressions, ϕ represents the nondimensionalized displacement function of a uniform beam subjected to a unit rotation at one end, as shown in the figure.

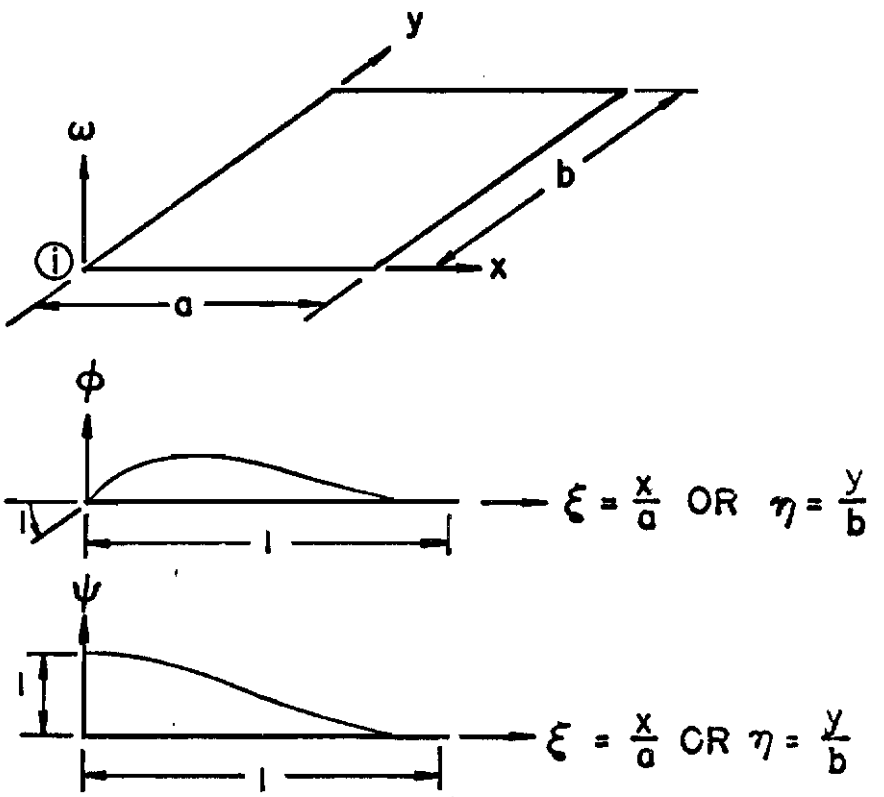

Figure 1. Plate Bending Displacement Functions

Similar displacement functions may be used to represent the deformations resulting from unit nodal displacements introduced at each of the corners. The resulting set of 12 displacement patterns provides for complete compatibility of displacements and slopes between adjacent elements. The displacement functions include terms as high as the 6th degree in x and y; unfortunately, however, the uniform twist term ($w = a_5xy$) is not included in the approximation, thus the second requirement listed above is violated and this infinite element system does not converge to the correct results.

Approved for Public Release

Contrails

Triangular Elements

1. (A) Polynomial series expressions in x and y also have formed the basis for several types of displacement patterns used in the analysis of triangular element stiffnesses. Adini (Reference 18) suggested the following form:

$$W = \alpha_1 + \alpha_2 x + \alpha_3 y + \alpha_4 x^2 + \alpha_5 y^2 + \alpha_6 x^3 + \alpha_7 x^2 y + \alpha_8 x y^2 + \alpha_9 y^3 \quad (11)$$

It will be noted that only 9 terms are included, corresponding with the 9 degrees of freedom of the triangular plate. The complete polynomial series includes 10 terms up to the cubic elements; Adini chose to omit the uniform twist term from his expression in order to maintain symmetry.

2. (T) The Adini displacement function (Equation 11) has an obvious defect in the omission of the uniform twist term. Tocher (Reference 12) tried two other assumptions in attempting to obtain an improved triangular plate bending element. The first of these is represented by the following displacement function:

$$W = \alpha_1 + \alpha_2 x + \alpha_3 y + \alpha_4 x^2 + \alpha_5 xy + \alpha_6 y^2 + \alpha_7 x^3 + \alpha_8 (x^2 y + xy^2) + \alpha_9 y^3 \quad (12)$$

The symmetry of this expression has been maintained by combining two of the cubic terms into a single coordinate.

3. (T-10) Tocher's second element stiffness approximation (Reference 11) was obtained by assuming the complete 10-term polynomial displacement expression and then reducing to a 9-degree of freedom system by the Ritz method (References 12 and 13). This procedure has the advantage of producing a stiffness matrix which is invariant with regard to the orientation of the element in the x-y plane; however, the element flexibility is greatly increased in the process.

4. (HCT) Although each of the above described triangular element displacement functions provides for displacement compatibility between adjacent elements, they do not provide normal slope compatibility along the edges. It is somewhat awkward to achieve full slope and displacement compatibility in a triangular plate bending system; however, this result can be achieved by dividing the elements into 3 subtriangles. This concept was first suggested by T. K. Hsieh in correspondence with the senior author, and the procedure for deriving the element stiffness was developed by the authors.

A general triangular element, with its three element subdivisions is shown in Figure 2. The interior point "o" may be located arbitrarily, but in the present discussion it will be assumed at the center of gravity of the area. It should be noted that additional nodal points t, u, v, have been located at the midpoints of the interior sub-element boundaries.

The stiffness analysis is based on assuming an independent polynomial displacement expression for each of the sub-elements. For example, for sub-element a, which is shown in Figure 3, the displacement functions are expressed in terms of the $\bar{x}$, $\bar{y}$ coordinate system, in which the $\bar{x}$ axis is directed parallel with the exterior side of the sub-element. A different

Approved for Public Release

Contrails

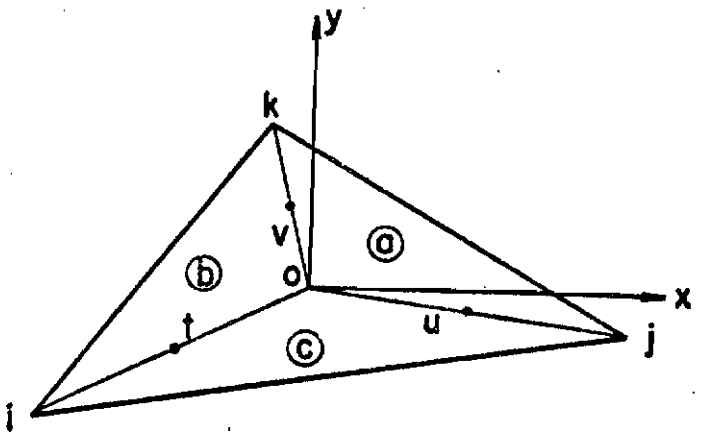

Figure 2. Triangular Element with Sub-Elements

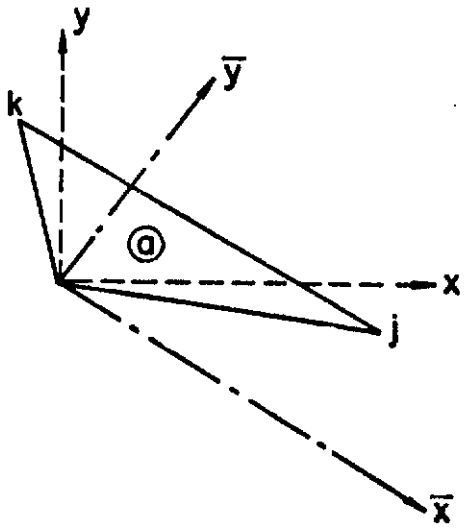

Figure 3. Coordinate System for Sub-Element a

Approved for Public Release

Contrails

coordinate system of this type applies to each sub-element. The displacements of sub-element a are assumed to be given by:

$$\overline{W}_a = \alpha_1 + \alpha_2 \bar{x} + \alpha_3 \bar{y} + \alpha_4 \bar{x}^2 + \alpha_5 \bar{x}\bar{y} + \alpha_6 \bar{y}^2 + \alpha_7 \bar{x}^3 + \alpha_8 \bar{x}\bar{y}^2 + \alpha_9 \bar{y}^3 \tag{13}$$

or symbolically

$$\overline{W}_a = M_a \alpha_a \tag{13a}$$

It will be noted that the term depending on $\bar{x}^2\bar{y}$ has been excluded from the expression, thus the normal slope may vary only linearly along the exterior boundary. It is this limitation which ensures slope compatibility in the resulting element system.

An expression similar to Equation 13 is assumed for each sub-element; thus the displacements of the complete element involve a total of 27 generalized coordinates α. Eighteen of these are employed in satisfying internal compatibility requirements between the adjacent sub-elements, while the remaining 9 are related to the 9 degrees of freedom of the complete element.

The process of reduction from 27 to 9 degrees of freedom in the displacement functions may be explained most easily as follows. First the corner displacements and slopes are evaluated in each sub-element, in the local sub-element coordinate system, and then transformed to the global (x, y) coordinate system. The result is a set of expressions for the displacements and slopes at the corners of each of the sub-elements. The vector representing the displacement and slopes at corner i in sub-element c may be written:

$$\begin{bmatrix} W \\ W_{,x} \\ W_{,y} \end{bmatrix}_i^c \equiv r_i^c = A_i^c \alpha_c \tag{14}$$

Similar expressions may be written for the other corners and sub-elements. The following set of compatibility relationships may then be established:

$$\begin{bmatrix} r_i \\ r_j \\ r_k \\ r_i^c \\ r_j^a \\ r_k^b \\ r_o^a \\ r_o^b \end{bmatrix} = \begin{bmatrix} r_i^c \\ r_j^a \\ r_k^b \\ r_i^b \\ r_j^c \\ r_k^a \\ r_o^b \\ r_o^c \end{bmatrix} \tag{15}$$

Approved for Public Release

Contrails

in which the superscripts refer to the sub-elements. Symbols without superscripts refer to the nodal displacements of the complete element.

Since each vector represents 3 displacement quantities, there are 24 algebraic equations contained in matrix Equation 15. The first 9 merely state that the nodal displacements in the complete element correspond with the sub-element displacements at the appropriate corners. The remaining 15 equations define the equality of nodal displacements in adjacent elements at the corners i, j, k, and o. In order to establish slope compatibility along the interior edges of the sub-elements, however, additional constraints must be imposed. For this purpose, the normal slope at point t of sub-element c is evaluated from the displacement functions and written:

$$(W,n)_t^c \equiv r_t^c = A_t^c \alpha_c \tag{16}$$

Similar expressions may be written for the other interior points u and v, and for the other sub-elements. The three conditions imposing compatibility of slopes between the sub-elements then are as follows:

$$\begin{bmatrix} r_t^c \\ r_u^a \\ r_v^b \end{bmatrix} = \begin{bmatrix} r_t^b \\ r_u^c \\ r_v^a \end{bmatrix} \tag{17}$$

Now making use of expressions of the types of Equations 14 and 16, the complete set of compatibility conditions of Equations 15 and 17 take the form

$$\begin{bmatrix} r_i \\ r_j \\ r_k \\ 0 \\ 0 \\ 0 \\ 0 \\ 0 \\ 0 \\ 0 \\ 0 \end{bmatrix} = \begin{bmatrix} 0 & 0 & A_i^c \\ A_j^a & 0 & 0 \\ 0 & A_k^b & 0 \\ 0 & -A_i^b & A_i^c \\ A_j^a & 0 & -A_j^c \\ -A_k^a & A_k^b & 0 \\ 0 & A_o^b & -A_o^c \\ A_o^a & -A_o^b & 0 \\ 0 & -A_t^b & A_t^c \\ A_u^a & 0 & -A_u^c \\ -A_v^a & A_v^b & 0 \end{bmatrix} \begin{bmatrix} \alpha_a \\ \alpha_b \\ \alpha_c \end{bmatrix} \tag{18}$$

Approved for Public Release

Contrails

Symbolically, Equation 18 may be written:

$$\begin{bmatrix} \frac{r}{0} \end{bmatrix} = \begin{bmatrix} A_{aa} & A_{ao} \\ A_{oa} & A_{oo} \end{bmatrix} \begin{bmatrix} \alpha_a \\ \alpha_o \end{bmatrix} \tag{18a}$$

in which the first 9 rows and columns of the 27 x 27 compatibility matrix have been partitioned out. An expression relating the nine generalized coordinates of element a to the nine nodal displacements of the complete element may then be written:

$$r = \left(A_{aa} - A_{ao} A_{oo}^{-1} A_{oa} \right) \alpha_a \equiv \bar{A} \alpha_a \tag{19}$$

From this, the generalized coordinates may be expressed in terms of the nodal displacements by the inversion:

$$\alpha_a = \bar{A}^{-1} r \tag{20}$$

The remaining generalized coordinates may be expressed in terms of these 9 by means of the relationships expressed in Equation 18a:

$$0 = A_{oa} \alpha_a + A_{oo} \alpha_o \tag{21}$$

i.e.,

$$\alpha_o = -A_{oo}^{-1} A_{oa} \alpha_a$$

Then the entire set of generalized coordinates may be expressed in terms of the nodal displacements as follows:

$$\begin{Bmatrix} \alpha_a \\ \alpha_o \end{Bmatrix} = \begin{bmatrix} \bar{A}^{-1} \\ -A_{oo}^{-1} A_{oa} \bar{A}^{-1} \end{bmatrix} r \equiv \bar{\bar{A}}^{-1} r \tag{22}$$

Now the nodal stiffness of the element may be obtained by evaluating first the generalized coordinate stiffness $\bar{k}$ of the set of three sub-elements, involving all 27 generalized coordinates. The transformation matrix of Equation 22 then serves to transform to the desired 9 x 9 nodal stiffness expression:

$$k = \bar{\bar{A}}^{-1} \bar{k} \bar{\bar{A}}^{-1} \tag{23}$$

CONVERGENCE OF THE FINITE ELEMENT APPROXIMATIONS

In order to evaluate the relative merit of these seven rectangular and triangular element stiffness matrices, a series of comparative analyses were carried out. The most extensive investigation was on a set of uniform rectangular plates. Eight different plates were considered involving two different aspect ratios, two edge support conditions, and two loading conditions. The plate geometry and schedule of cases considered are shown in Figure 4.

Each of these eight cases was analyzed by the finite element procedure, using the 3 rectangular and 4 triangular element stiffness matrices derived from the above described sets of displacement functions. Because of the double symmetry of the plate, only one quarter of it

Approved for Public Release

Contrails

was considered in the analyses. The convergence of the finite element procedure was studied by using a series of different element mesh sizes in the analysis of each case. Typical finite element mesh arrangements are shown in Figure 5. An additional 6 by 6 arrangement (n = 6) also was used. The rectangular element mesh arrangements were the same as the triangular with the diagonal dividing lines omitted. It should be noted that the mesh number "n" refers to the number of rectangles along the side of one-quarter of the complete plate. The complete schedule of investigations involved 280 different analyses.

Results of the convergence studies are presented in Figure 6 through 13. In this investigation the deflection of the center of the plate was taken as the measure of the quality of the approximation, and these figures show how the central deflection varies with mesh size for each of the different finite element systems.

The quantity plotted in these figures is the deflection coefficient, a dimensionless number proportional to the computed central deflection. In the case of the uniformly loaded plates, this coefficient is designated by α, and the central deflection is given by

$$W_c = \alpha \frac{q a^4}{D}$$

where D is the flexural rigidity factor and q represents the load intensity. For the concentrated load cases, the deflection coefficient is designated β, and the central deflection is given by

$$W_c = \beta \frac{P a^2}{D}$$

where P is the concentrated load. It should be noted that the uniform loading was approximated in the finite element analysis by a set of concentrated nodal forces. In this investigation, these equivalent forces were established on the basis of assumed tributary areas, and consisted only of vertical loads. More complex sets of equivalent forces, including nodal moments, could have been developed by virtual work principles, but the simpler procedure was considered satisfactory for the comparative studies involved here.

Two graphs are included in each figure: the results for the rectangular elements are shown on the upper graph and those for the triangular elements are shown in the lower graph. Also included in the upper graph are the results for the compatible triangle elements, to demonstrate how well the best of the triangular elements compare with the rectangular elements. It should be noted that the two types of graphs are plotted to different scales because the results obtained with the rectangular elements are generally much better than the triangular element results.

Examination of these graphs reveals that the best results generally are given by the Melosh triangle elements (M), while the next best results are obtained with the twelve-term polynomial rectangular elements (ACM). Only in the simply supported, uniformly loaded cases is this order of preference reversed. The third best results are obtained generally with the compatible triangle elements (HCT) for the fine mesh systems. These elements give relatively poor results for the very coarse mesh systems, being much too stiff in these cases, but for any reasonably fine mesh system they are by far the best of the triangular elements, and generally better than the compatible rectangle elements (P).

Certain significant characteristics of the various finite element systems are evident in these figures. For example, it is clear that the triangular elements based on the 10-term polynomial (T-10) are far too flexible in all cases, and tend to converge toward a central deflection which is much too large. Conversely, the triangular elements from which the principal cubic term has been omitted (A) are too stiff in most cases, and tend to underestimate the

Approved for Public Release

Contrails

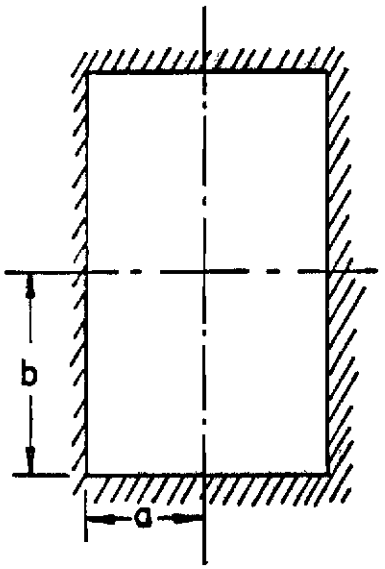

CASE	b/a	EDGES	LOAD
1	1	SS	U
2	2	SS	U
3	1	C	U
4	2	C	U
5	1	SS	C
6	2	SS	C
7	1	C	C
8	2	C	C

EDGES : SIMPLY SUPPORTED (SS) OR CLAMPED (C)

LOADING : UNIFORM (U) OR CONCENTRATED AT CENTER (C)

Figure 4. Schedule of Rectangular Plate Analyses

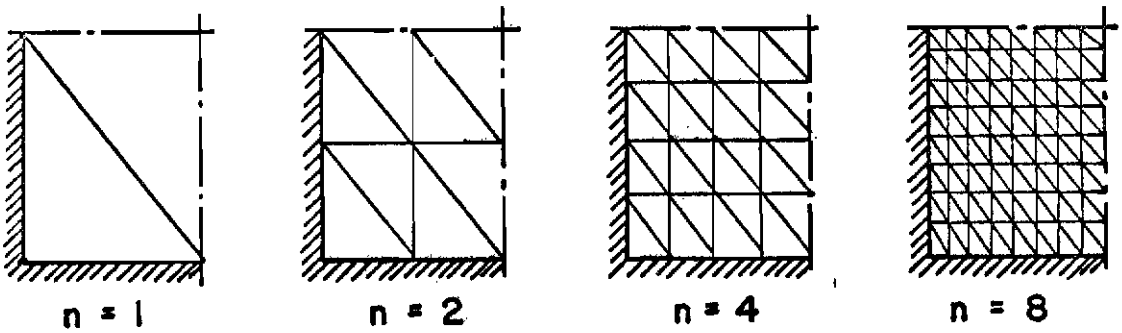

Figure 5. Typical Finite Element Idealizations

Approved for Public Release

Contrails

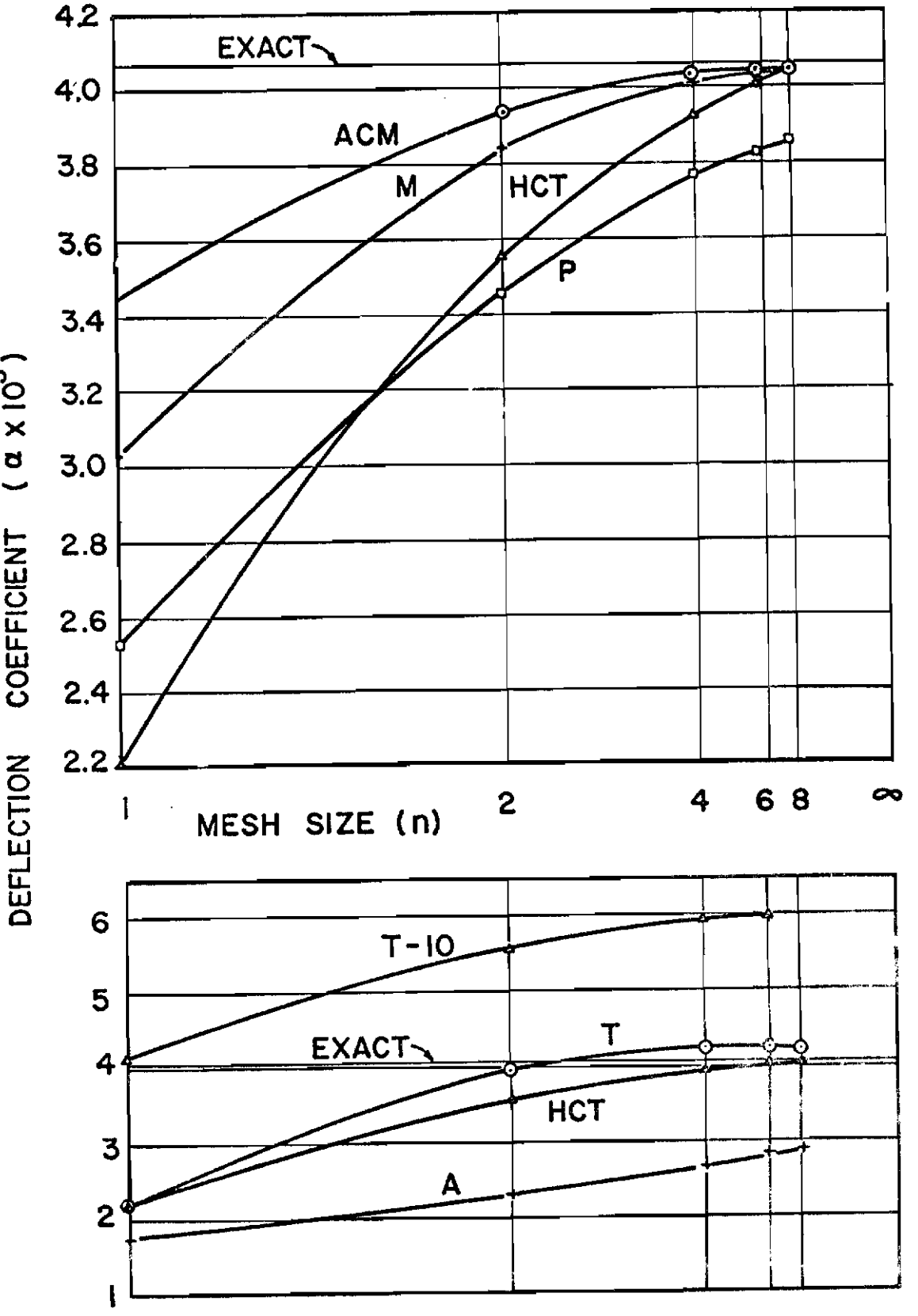

Figure 6. Central Deflection of Rectangular Plate Case 1 (1-SS-U)

Approved for Public Release

Contrails

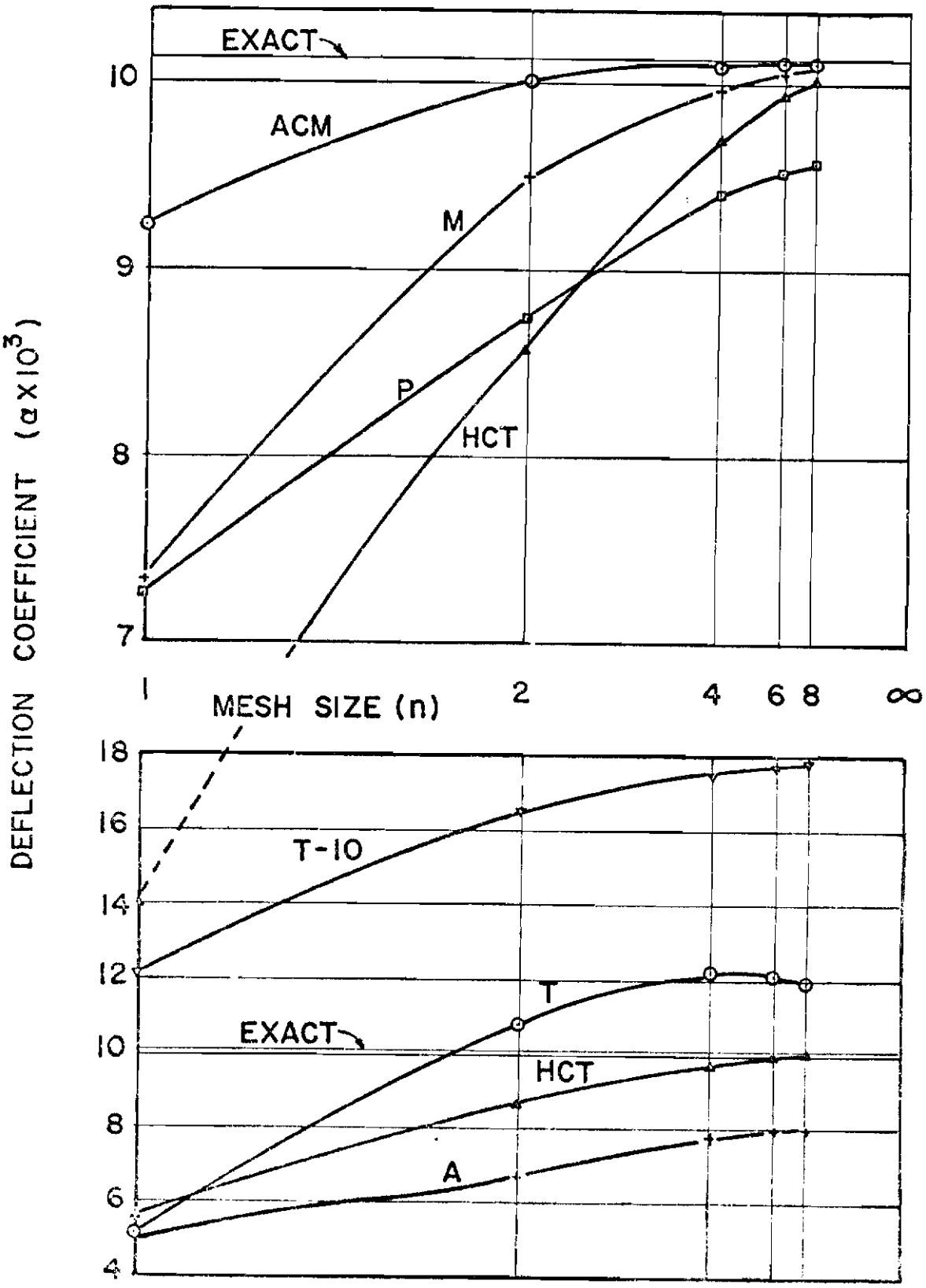

Figure 7. Central Deflection of Rectangular Plate Case 2 (2-SS-U)

Approved for Public Release

Contrails

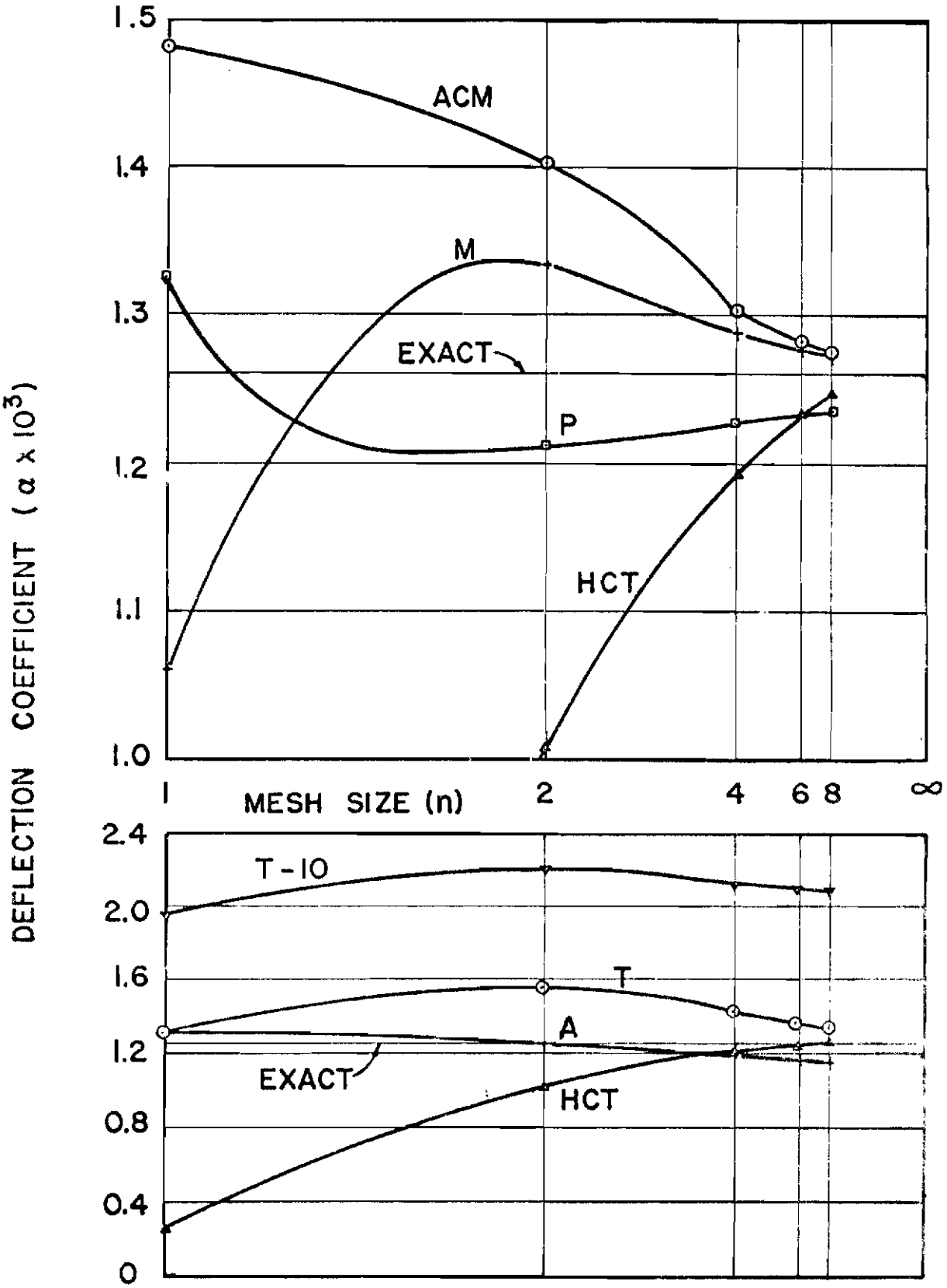

Figure 8. Central Deflection of Rectangular Plate Case 3 (1-C-U)

Approved for Public Release

Contrails

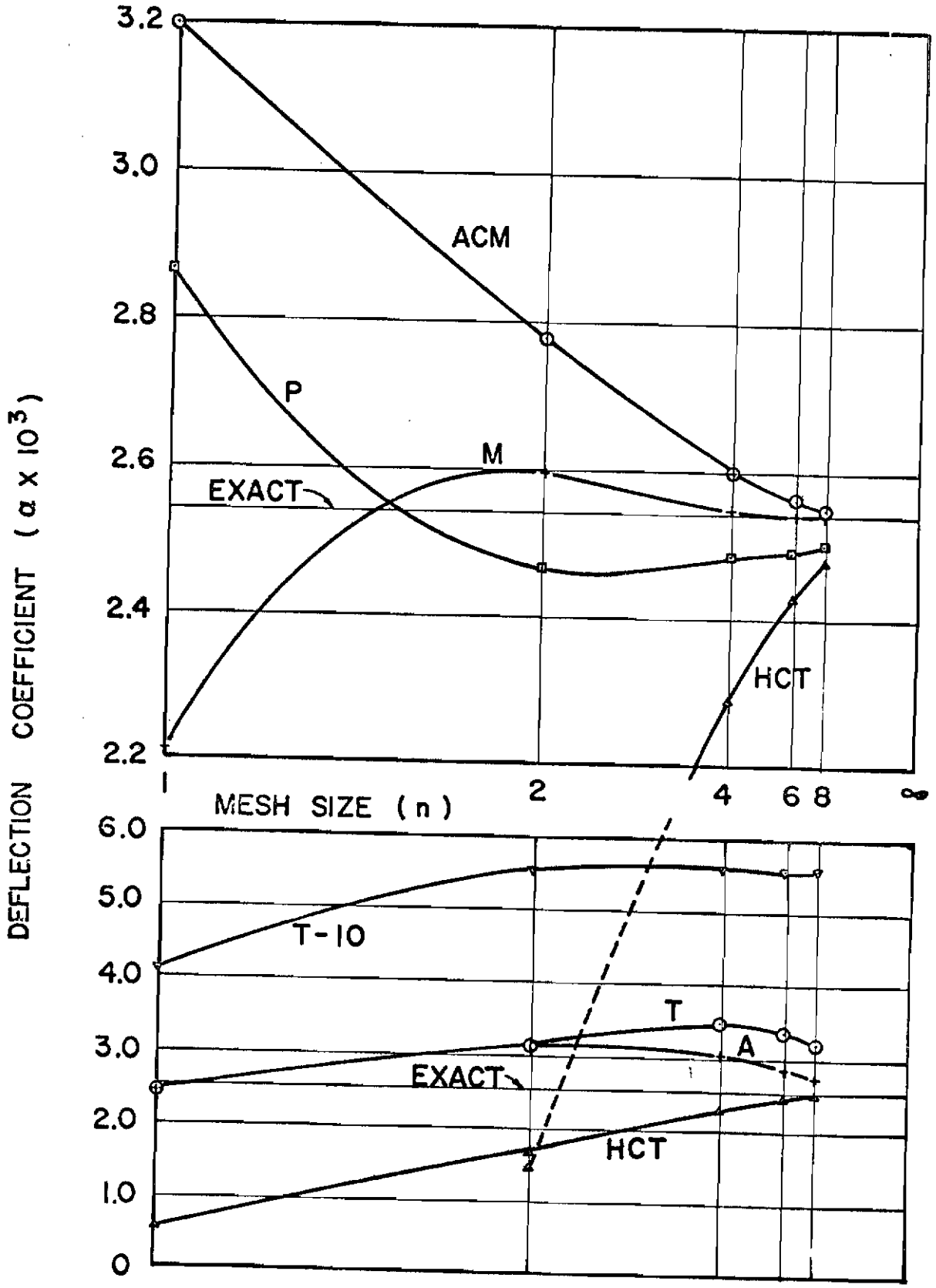

Figure 9. Central Deflection of Rectangular Plate Case 4 (2-C-U)

Approved for Public Release

Contrails

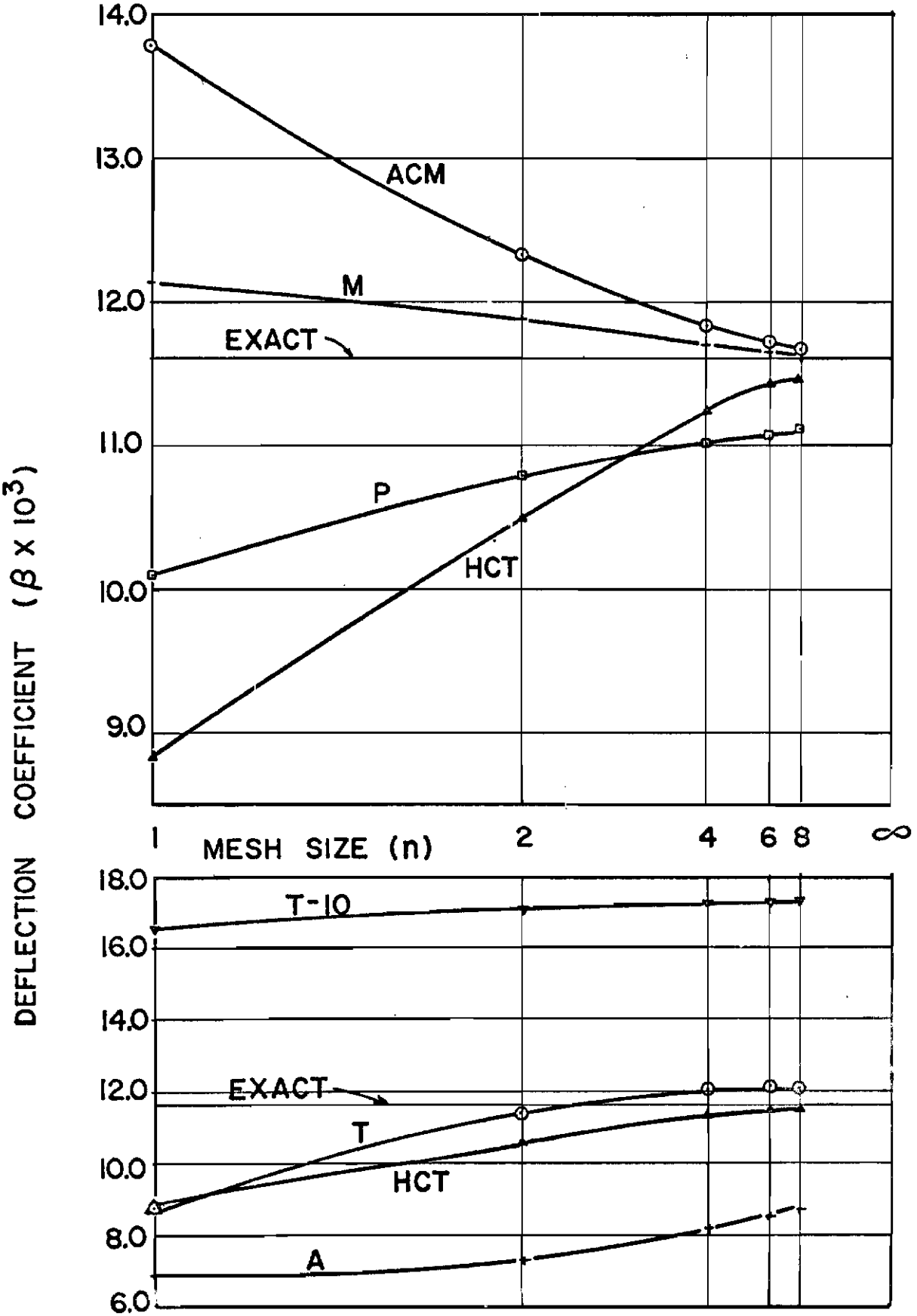

Figure 10. Central Deflection of Rectangular Plate Case 5 (1-SS-C)

Approved for Public Release

Contrails

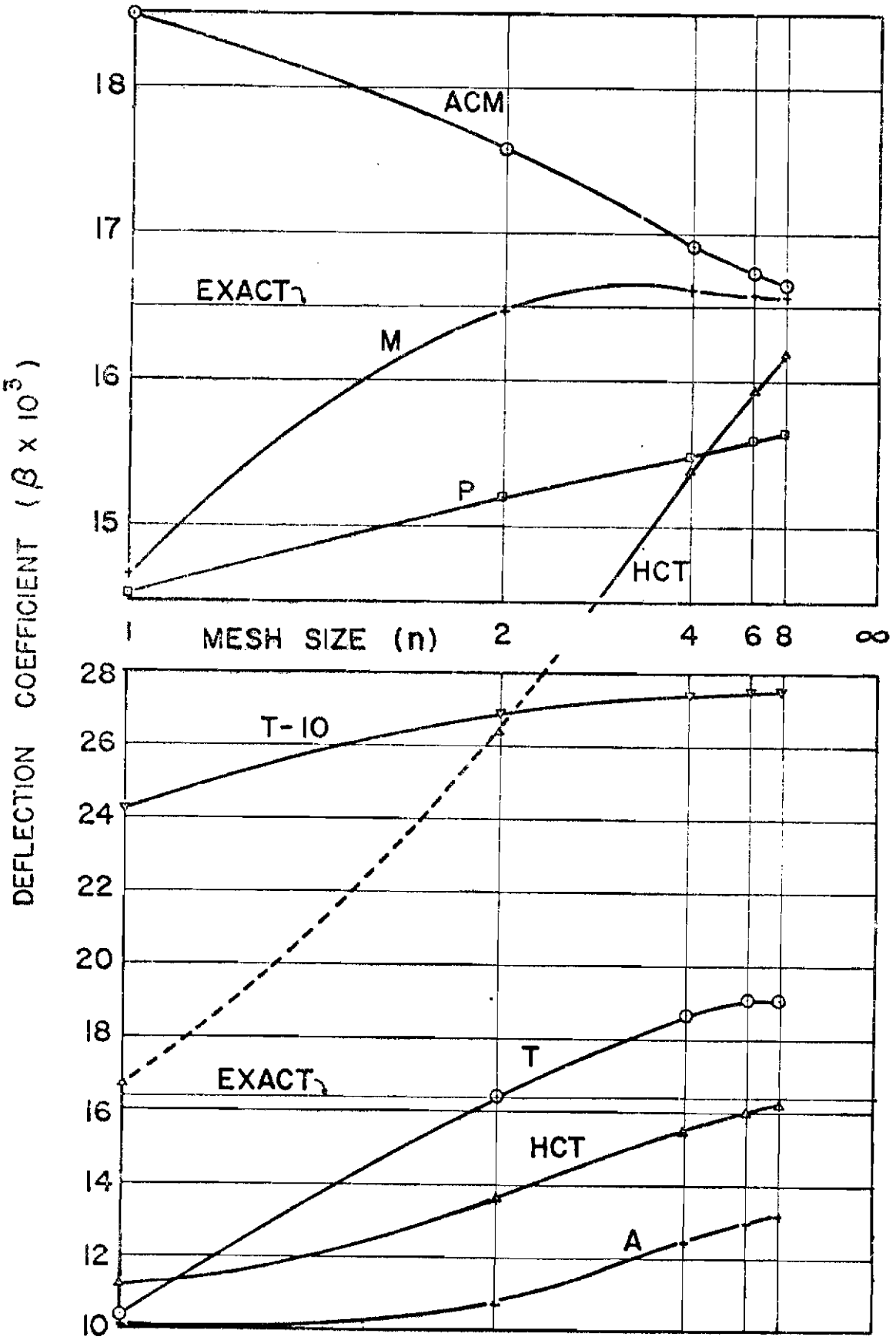

Figure 11. Central Deflection of Rectangular Plate Case 6 (2-SS-C)

Approved for Public Release

Contrails

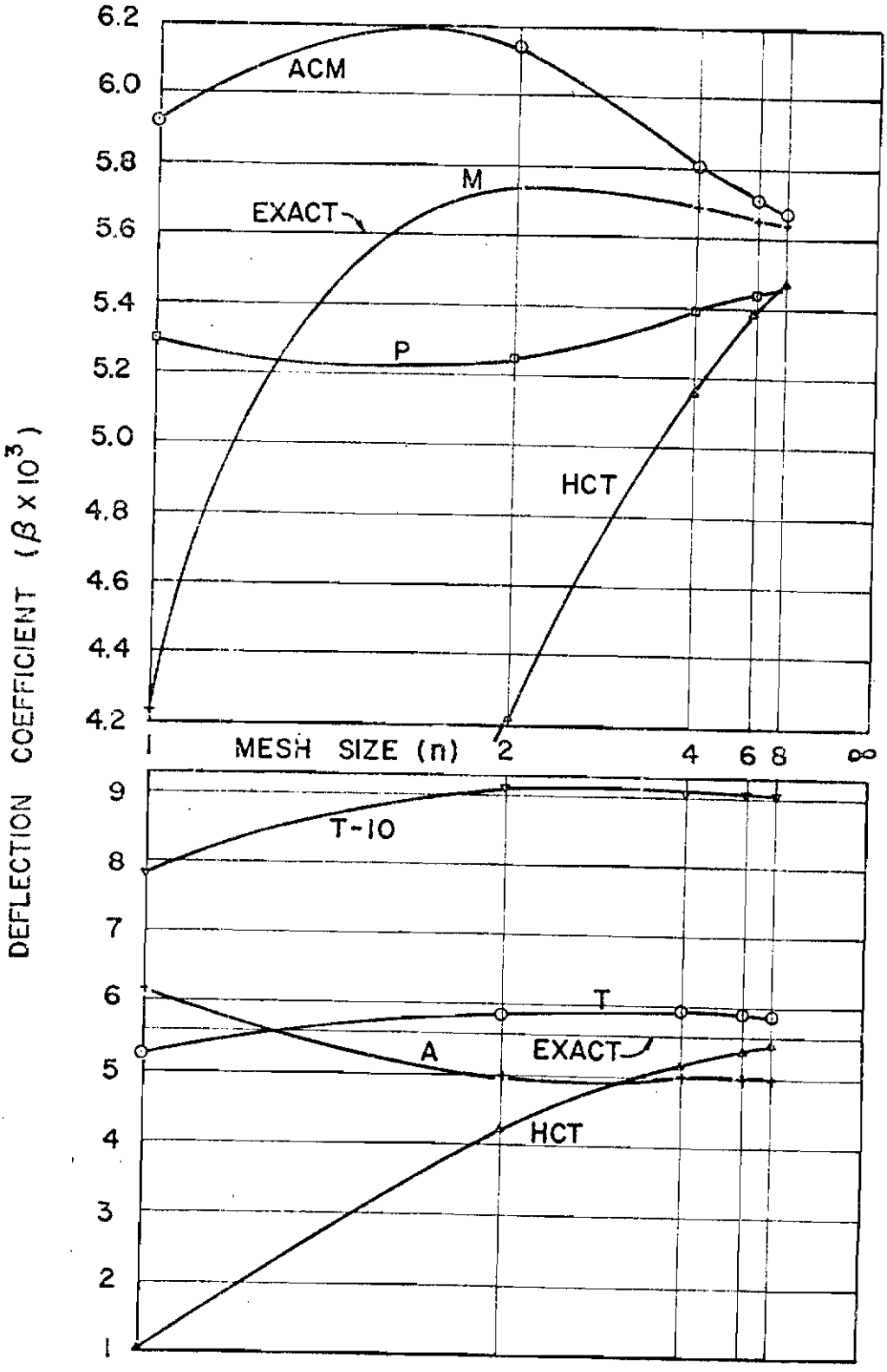

Figure 12. Central Deflection of Rectangular Plate Case 7 (1-C-C)

Approved for Public Release

Contrails

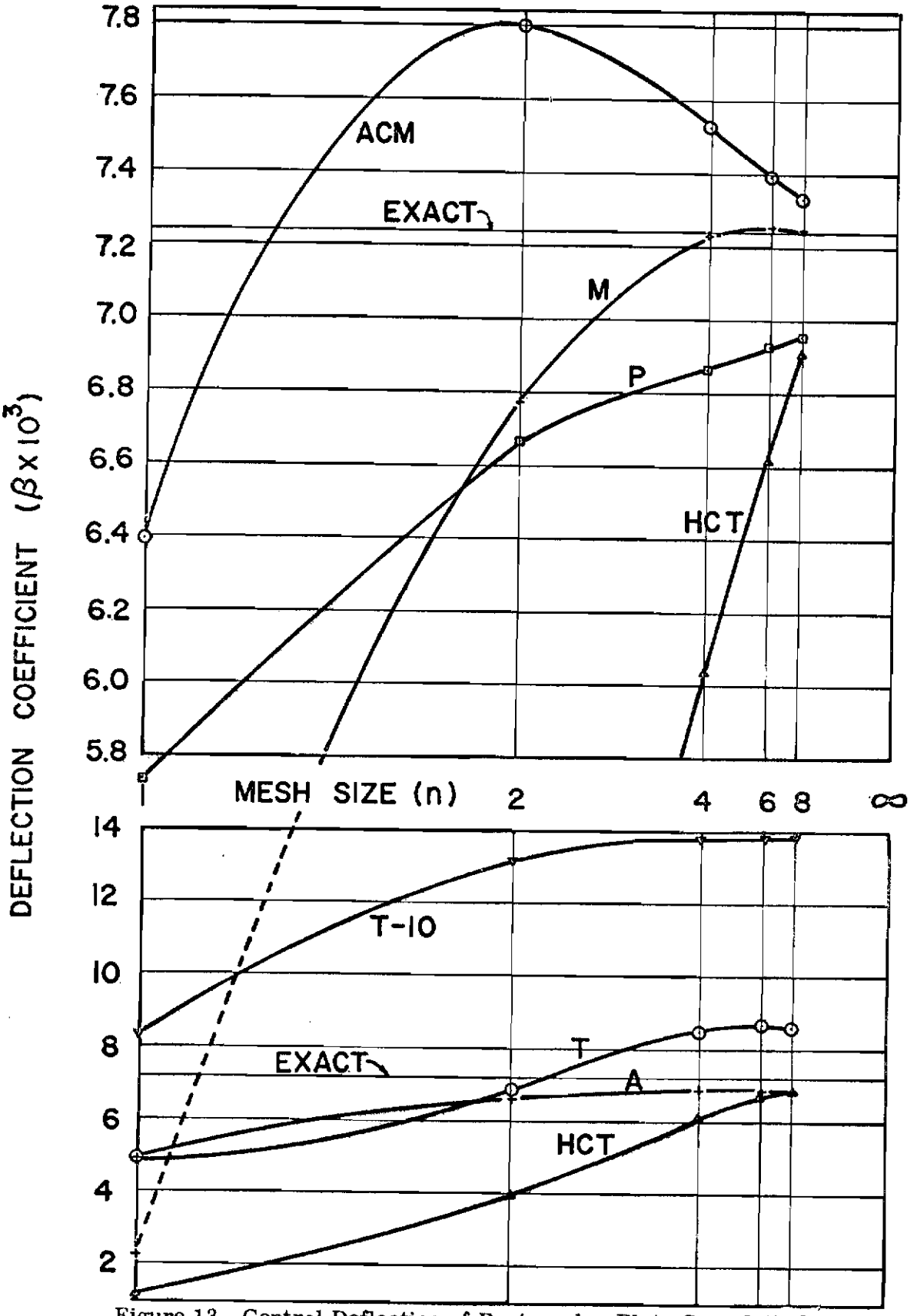

Figure 13. Central Deflection of Rectangular Plate Case 8 (2-C-C)

Approved for Public Release

Contrails

central deflection. This element seems to give better results in approximating the plate system with clamped edges, but does not converge toward the correct result even in these cases. In fact the only triangular element which does converge toward the correct answer is the compatible triangle (HCT), and it demonstrates monotonic convergence in all cases. This type of behavior is to be expected, of course, because the displacement functions used in defining the stiffness of this element satisfy the three requirements listed above.

In this connection, it is of interest to note that none of the rectangular elements satisfies these requirements. The elements (ACM) and (M) do not maintain edge slope compatibility and therefore may be overly flexible or overly stiff, i.e., they may converge toward the correct result either from above or below. Both of these elements appear to possess satisfactory convergence characteristics, although they do not necessarily converge monotonically. The compatible rectangular elements (P), which exclude uniform twist deformations, are found to be somewhat too stiff even for very fine mesh cases, i.e., they appear to converge to an overly stiff result.

SUPPLEMENTARY INVESTIGATIONS

Rectangular Plate Bending Moments

In addition to study of the nodal displacements, it is of interest to consider the distribution of internal moment predicted by the finite element procedure. The internal moments were studied in detail only for one plate system, the simply supported, uniformly loaded plate with the aspect ratio of 2 (Case 2). Only two finite element approximations were used in this study, the rectangular element (ACM) which gave the best results of all for this case and the compatible triangular element (HCT). In the rectangular elements, the internal moments were found by finite difference operations on the computed nodal displacements, while a moment transformation matrix based on the assumed displacement functions was used with the triangular elements. In this case, the nodal moments were taken as the average of all of the sub-element moments computed at the specific node.

Results of this study are presented in Figure 14, which gives the exact M_x moment variation along the centerline of the plate as well as the result of the two finite element approximations. It will be noted that the moment values obtained from the rectangular element system provided a good approximation to the actual distribution for all mesh sizes. For n = 8 the calculated results are indistinguishable from the theoretical values, while for the coarser meshes, the results are one essentially straight line segment approximations of the correct distribution. In effect, this merely is a demonstration of the accuracy of the nodal displacement analyses since the moments were derived directly from these displacements by finite difference formulas. On the other hand, the triangular element approximation gave low values for the moments in all mesh sizes, but with results tending to converge toward the true values as the mesh size is reduced. These discrepancies vary somewhat in proportion to the error in central deflection, but the errors are somewhat larger toward the edges than at the center for all mesh sizes.

Twisting of Square Plate

Another supplementary study, intended to provide greater emphasis on the twisting behavior of the finite elements, involved analysis of deflections in a square plate subjected to pure twist. The plate was assumed to be simply supported at three corners and subjected to a vertical load at the fourth corner, as shown in Figure 15. The plate was divided into an 8 by 8 square mesh, and deflections were calculated for each of the seven different element types considered in this investigation.

Approved for Public Release

Contrails

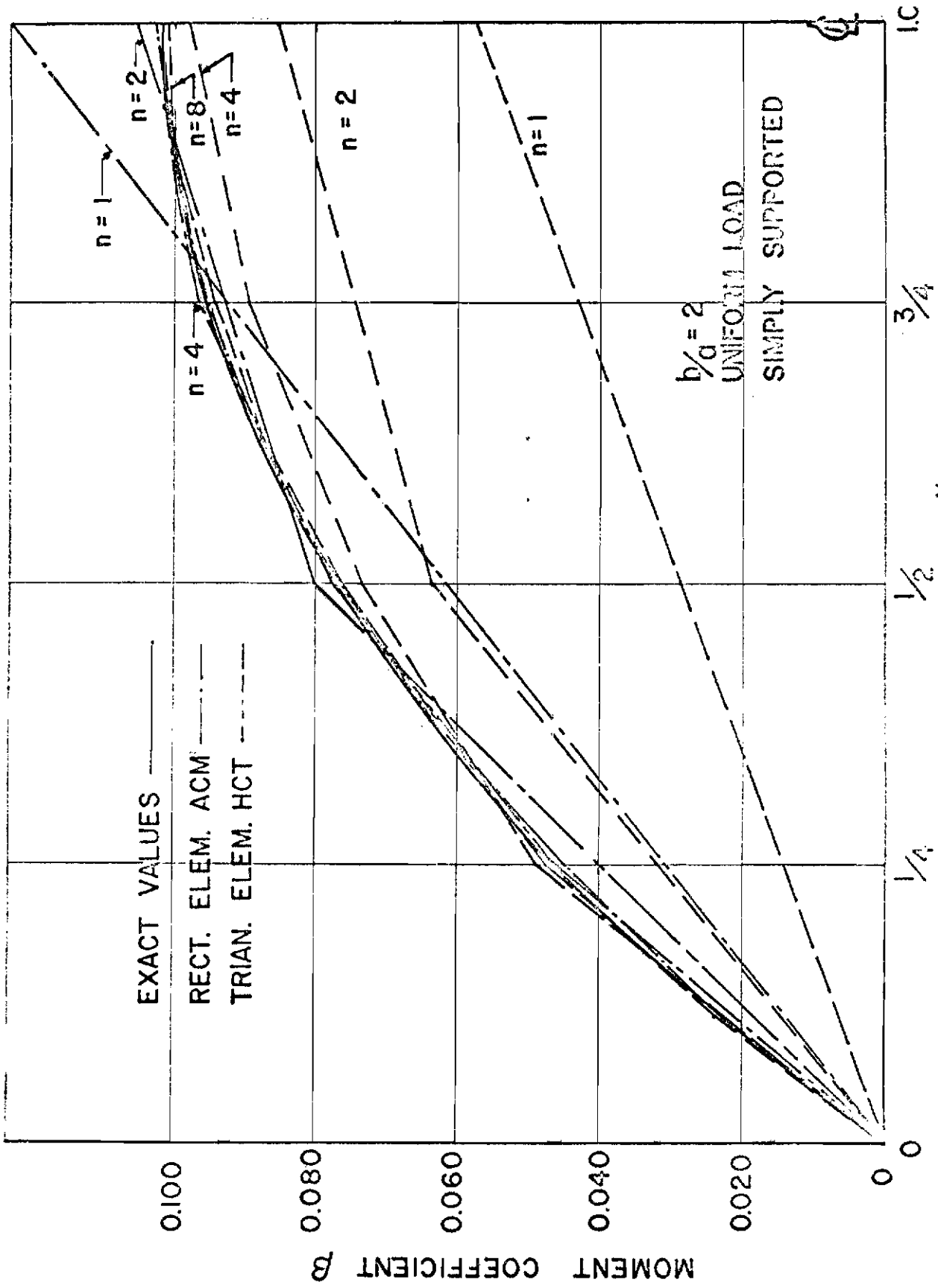

Figure 14. Moment M_x on Centerline of Plate, Case 2

Approved for Public Release

Contrails

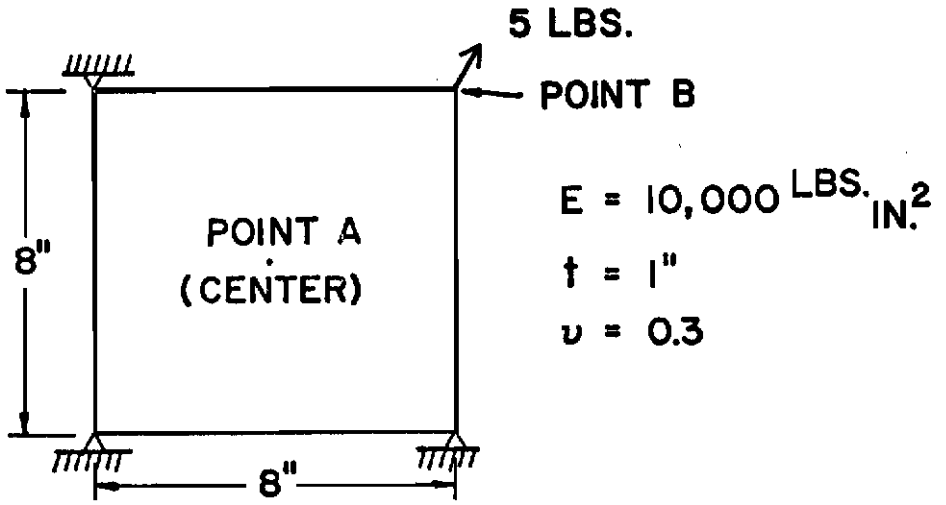

ELEMENT TYPE	DEFLECTION AT POINT A	DEFLECTION AT POINT B
ACM	0.06244	0.24972
M	0.06252	0.24998
P	0.05552	0.22208
A	0.04154	0.13897
T	0.06279	0.25830
T-10	0.04848	0.31391
HCT	0.06254	0.25002
EXACT	0.06240	0.24960

Figure 15. Twisting Deflections in Square Plate

Approved for Public Release

Contrails

The deflections calculated at the midpoint and at the loaded corner for each type of element are tabulated in the figure, together with the theoretical values. These results are seen to be equivalent to those noted earlier. The most accurate representations are given by the ACM and M rectangles, while the compatible triangles are seen to be nearly as good. The compatible rectangles, (P), however, are considerably too stiff in this case, due to their omission of the principal twisting term in the displacement functions. The triangles, T, give reasonably good results in this case while the other triangles are found again to be completely unreliable.

Rhombic Cantilever Plate

A final, rather general, comparison of element effectiveness was given by the analysis of a rhombic cantilever plate subjected to uniform load. Experimental studies of this plate (Reference 18) provided results against which the finite element analyses could be compared. In all of these analyses, a 1-1/2-inch square element size was the basis of the idealizations, leading to an 8 x 6 mesh, in which the outboard row of elements was narrower than standard. The sloping boundaries of the plate were treated as stepped in the rectangular element analyses while the triangular element system fitted the boundaries exactly.

A sketch of the plate and the finite element layout is shown in Figure 16. Experimental results were measured at the nodes designated 1 through 6, so the finite element displacements were obtained for these same points by interpolation of the nodal point deflection data. The results are tabulated in Figure 16; again the same relative accuracy is indicated for the various types of elements. As before the rectangular elements M and ACM give the best results, with the compatible triangles HCT in third place. None of the other element systems seems to warrant further consideration.

CONCLUSIONS

The results of this investigation demonstrate that two of the rectangular elements (M and ACM) and the compatible triangular element (HCT) provide very satisfactory analyses when used in the finite element analysis of plate bending. These two rectangular elements are somewhat more accurate than the triangular element, particularly when a coarse mesh idealization is used and therefore are to be recommended for the analysis of any system in which the boundaries fit the rectangular coordinate area. On the other hand the compatible triangle results are quite accurate when a reasonably fine mesh system is used, and this idealization has the advantage of monotonic convergence. Furthermore, these triangular elements are to be recommended for idealizations of plate systems with arbitrarily shaped boundaries, or in the analysis of doubly curved shell surfaces.

It is of interest to note that further improvement is possible in the compatible triangle if one is willing to employ additional nodal points in defining its degrees of freedom. For example, a 12-degree of freedom triangular element has been developed in which the three additional degrees of freedom are represented by the normal slopes at the midpoints of the sides. In this case, a complete 10-term polynomial expression may be assumed for the displacement functions of each sub-element, and the normal slopes along the boundaries of the element may vary quadratically rather than linearly (as was the case with element HCT).

Results obtained with this refined compatible element are noticeably improved over the HCT element, but are not reported herein because a 12-degree of freedom triangle cannot be compared directly with a 9-degree system. Still further refinement might be achieved through the selection of additional element nodal degrees of freedom and the assumption of additional terms in the polynomial displacement functions. However, it is doubtful that one should seek improved accuracy in a plate bending analysis by developing greater refinement in the finite element stiffness matrix; probably it would be better to use a simpler element with a finer mesh idealization.

Approved for Public Release

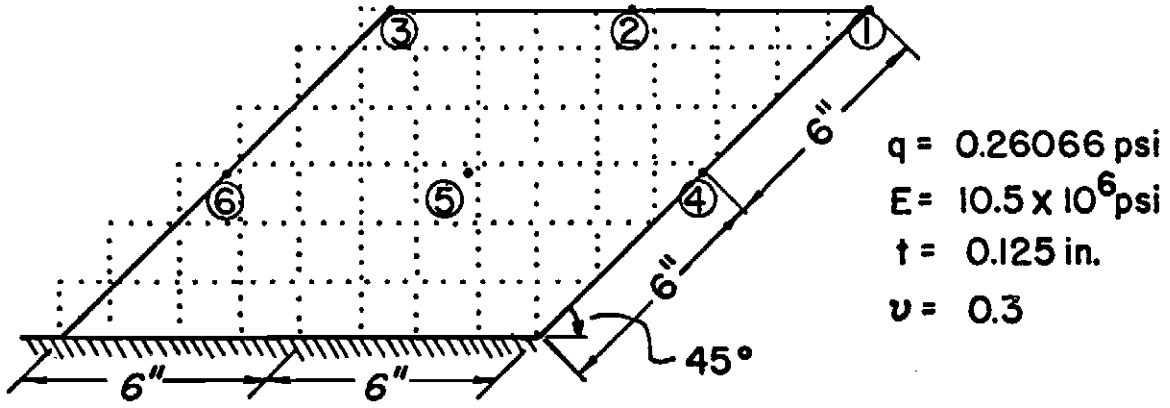

ELEMENT TYPE	DEFLECTION AT POINT 1	POINT 2	POINT 3	POINT 4	POINT 5	POINT 6
ACM	0.2962	0.1979	0.1135	0.114	0.052	0.0197
M	0.2938	0.1965	0.1181	0.113	0.051	0.0198
P	0.2786	0.1874	0.1155	0.108	0.050	0.0210
A	0.2565	0.1702	0.1048	0.1057	0.0467	0.0203
T	0.2784	0.1835	0.1046	0.1105	0.0471	0.0158
T-10	0.4211	0.2959	0.1990	0.1710	0.0821	0.0435
HCT	0.2814	0.1879	0.1108	0.1112	0.0491	0.0182
EXPERIMENT	0.297	0.204	0.121	0.129	0.056	0.022

Figure 16. Deflection of Uniformly Loaded Rhombic Cantilever

Approved for Public Release

Contrails

ACKNOWLEDGEMENTS

This paper summarizes the results of over six years of investigation into the finite element analysis of plate bending. The authors have been supported in these studies by a number of agencies and organizations, including the National Science Foundation (Grants G-7337 and G-18986), the Norwegian Technical University, Trondheim, and Cambridge University, England. All of the analyses reported herein were carried out on the computer facility of the Boeing Company, Airplane Division, Renton, Washington.

REFERENCES

1. Turner, M. J., Clough, R. W., Martin, H. C., and Topp, L. J., "Stiffness and Deflection Analysis of Complex Structures," Journal of Aeronautical Sciences, 23, No. 9, 1956.

2. Clough, R. W., The Finite Element in Structural Mechanics, Stress Analysis, O. C. Zienkiewicz and G. S. Holister, Ed., John Wiley and Sons, Ltd., London, 1965.

3. Clough, R. W., and Rashid, Yusef, "Finite Element Analysis of Axi-symmetric Solids," ASCE Engineering Mechanics Division Journal, Vol. 91, No. EM-1, 1965.

4. Melosh, R. J., "A Stiffness Matrix for the Analysis of Thin Plates in Bending," Journal of Aeronautical Sciences, 28, 34, 1961.

5. Clough, R. W., and Tocher, J. L., "Analysis of Thin Arch Dams by the Finite Element Method," Proc., International Symposium on the Theory of Arch Dams, Southampton University, England, April 1964, Pergamon Press.

6. Zienkiewicz, O. C., and Cheung, Y. K., "Finite Element Method of Analysis for Arch Dam Shells, and Comparison with Finite Difference Procedures," Proc., International Symposium in the Theory of Arch Dams, Southampton University, England, April 1964.

7. Melosh, R. J., "Structural Analysis of Solids," ASCE Structural Division Journal, Vol. 89, No. ST-4, 1963.

8. Gallagher, R. H., Padlog, J., Bijlaard, P. P., "Stress Analysis of Heated Complex Shapes," ARS Journal, Vol. 32, No. 5, 1962.

9. Fraijs de Veubeke, B., "Displacement and Equilibrium Models in the Finite Element Method," Stress Analysis, O. C. Zienkiewicz and G. S. Holister, Ed., John Wiley and Sons, Ltd., London, 1965.

10. Irons, B. M. R., and Draper, K. J., "Inadequacy of Nodal Connections in a Stiffness Solution for Plate Bending," AIAA Journal, Vol. 3, No. 5, 1965.

11. Gallagher, R. H., "A Correlation Study of Methods of Matrix Structural Analysis," AGARDograph 69, 1962.

12. Tocher, J. L., "Analysis of Plate Bending Using Triangular Elements," Ph. D. Dissertation, California Univ., Berkeley, Calif., 1962.

13. Pian, T. H. H., "Derivation of Element Stiffness Matrices," AIAA Journal, Vol. 2, March 1962, No. 3, (See also G. C. Best, "Derivation of Element Stiffness Matrices," AIAA Journal, Vol. 2, No. 8, August 1964).

Approved for Public Release

Contrails

14. Adini, A., and Clough, R. W., "Analysis of Plate Bending by the Finite Element Method," Rpt. submitted to the Nat. Sci. Foundation, Grant G7337, 1960.

15. Melosh, R. J., "Basis for Derivation of Matrices for the Direct Stiffness Method," AIAA Journal, Vol. 1, 1631, 1963.

16. Melosh, R. J., "A Stiffness Matrix for the Analysis of Thin Plates in Bending," Journal of Aeronautical Sciences, Vol. 28, 34, 1961.

17. Papenfuss, S. W., "Lateral Plate Deflection by Stiffness Matrix Methods with Application to a Marquee," M. S. Thesis, Department of Civil Engineering, University of Washington, Seattle, Wash., December 1959.

18. Adini, A., "Analysis of Shell Structures by the Finite Element Method," Ph. D. Dissertation, Department of Civil Engineering, University of California, Berkeley, Calif., 1961.

19. Plass, H. J., Gaines, J. H., and Newsom, C. D., "Application of Reissner's Variational Principle to Cantilever Plate Deflection and Vibration Problems," Journal of Applied Mechanics, Vol. 29, No. 1, March 1962.

APPENDIX

RECTANGULAR FINITE ELEMENT STIFFNESS COEFFICIENTS

The complete 12 x 12 stiffness matrix of a rectangular finite element represents the nodal force deflection relationships as indicated in Figure A-1. This 12 x 12 matrix may be constructed from the 12 x 3 matrices associated with the displacements of each joint. Thus the stiffness properties of the element are completely defined by the 12 x 3 matrix associated with any joint i.

For any given joint i, the stiffness matrix can be represented as the sum of four 12 x 3 matrices $\mathbf{K}_a$, $\mathbf{K}_b$, $\mathbf{K}_c$ and $\mathbf{K}_d$: i.e., $\mathbf{K}_i = \mathbf{K}_a + \mathbf{K}_b + \mathbf{K}_c + \mathbf{K}_d$. These represent the energy contributions from the $(W_{,xx})^2$, $(W_{,yy})^2$, $(W_{xx}.W_{,yy})$ and $(W_{,xy})^2$ curvature terms, respectively. These four stiffness component matrices of the total element stiffness are presented on the following pages for the three rectangular elements considered in this investigation.

Approved for Public Release

Contrails

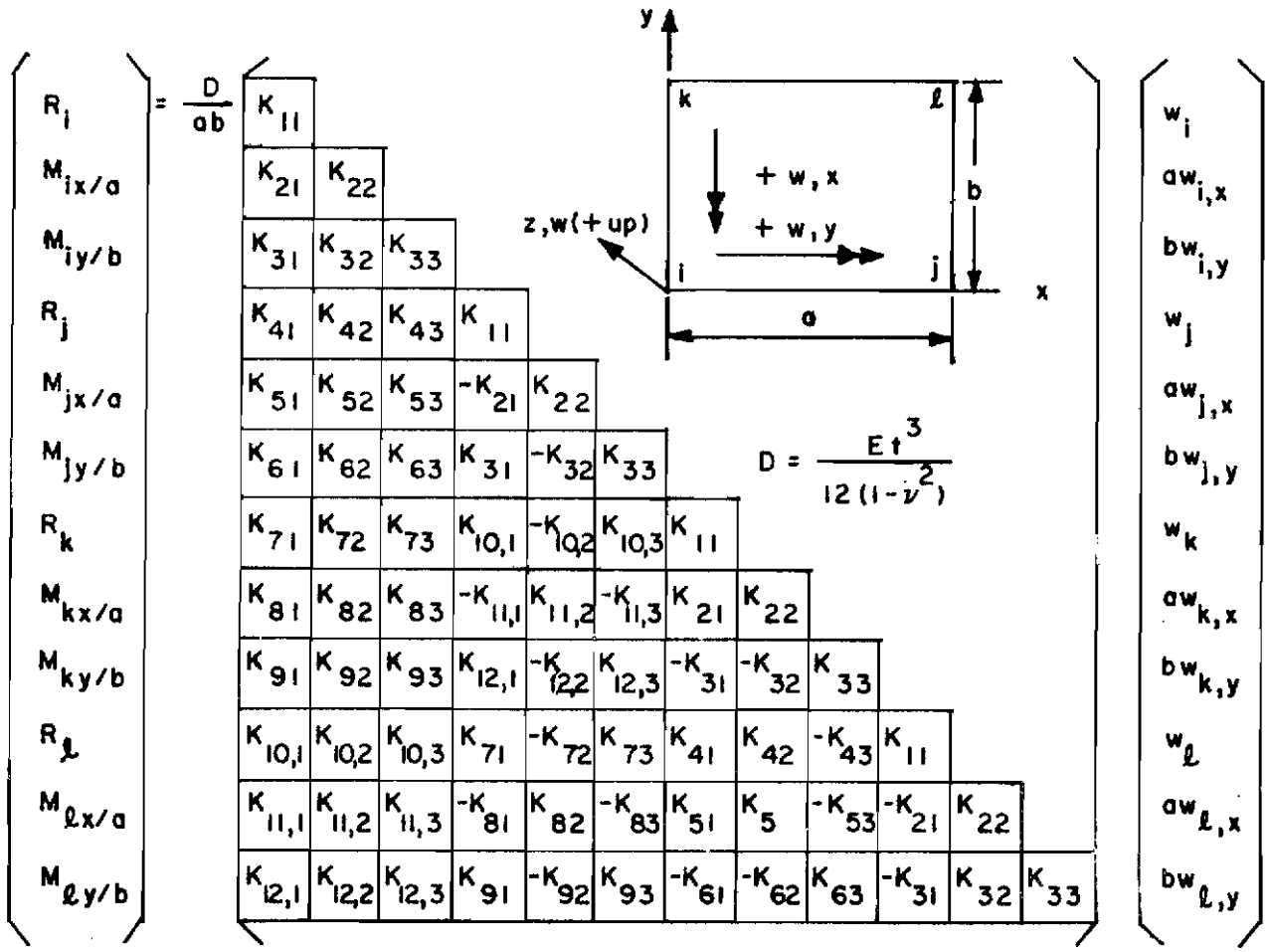

Figure A-1. Arrangement of Rectangular Stiffness Matrix

Approved for Public Release

Contrails

$$K_a = \frac{1}{70}\left(\frac{b}{a}\right)^2$$

312	156	44
156	104	22
44	22	8
-312	-156	-44
156	52	22
-44	-22	-8
108	54	26
54	36	13
-26	-13	-6
-108	-54	-26
54	18	13
26	13	6

$$K_b = \frac{1}{70}\left(\frac{a}{b}\right)^2$$

312	44	156
44	8	22
156	22	104
108	26	54
-26	-6	-13
54	13	36
-312	-44	-156
-44	-8	-22
156	22	52
-108	-26	-54
26	6	13
54	13	18

$$K_c = \frac{\nu}{50}$$

144	72	72
72	16	61
72	61	16
-144	-12	-72
12	-4	6
-72	-6	-16
-144	-72	-12
-72	-16	-6
12	6	-4
144	12	12
-12	4	-1
-12	-1	4

$$K_d = \frac{(1-\nu)}{50}$$

144	12	12
12	16	1
12	1	16
-144	-12	-12
12	-4	1
-12	-1	-16
-144	-12	-12
-12	-16	-1
12	1	-4
144	12	12
-12	4	-1
-12	-1	4

ELEMENT P

Approved for Public Release

Contrails

$$K_a = \left(\frac{b}{a}\right)^2$$

6	3	0
3	2	0
0	0	0
-6	-3	0
3	1	0
0	0	0
0	0	0
0	0	0
0	0	0
0	0	0
0	0	0
0	0	0

$$K_b = \left(\frac{a}{b}\right)^2$$

6	0	3
0	0	0
3	0	2
0	0	0
0	0	0
0	0	0
-6	0	-3
0	0	0
3	0	1
0	0	0
0	0	0
0	0	0

$$K_c = \frac{\nu}{16}$$

72	30	30
30	0	25
30	25	0
-72	-6	-30
6	0	5
-30	-5	0
-72	-30	-6
-30	0	-5
6	5	0
72	6	6
-6	0	-1
-6	-1	0

$$K_d = 2(1-\nu)$$

1	0	0
0	0	0
0	0	0
-1	0	0
0	0	0
0	0	0
-1	0	0
0	0	0
0	0	0
1	0	0
0	0	0
0	0	0

ELEMENT M

Approved for Public Release

Contrails

$$K_a = \frac{1}{3}\left(\frac{b}{a}\right)^2$$

12	6	0
6	4	0
0	0	0
-12	-6	0
6	2	0
0	0	0
6	3	0
3	2	0
0	0	0
-6	-3	0
3	1	0
0	0	0

$$K_b = \frac{1}{3}\left(\frac{a}{b}\right)^2$$

12	0	6
0	0	0
6	0	4
6	0	3
0	0	0
3	0	2
-12	0	-6
0	0	0
6	0	2
-6	0	-3
0	0	0
3	0	1

$$K_c = \nu$$

2	1	1
1	0	1
1	1	0
-2	0	-1
0	0	0
-1	0	0
-2	-1	0
-1	0	0
0	0	0
2	0	0
0	0	0
0	0	0

$$K_d = \frac{1-\nu}{15}$$

42	3	3
3	4	0
3	0	4
-42	-3	-3
3	-1	0
-3	0	-4
-42	-3	-3
-3	-4	0
3	0	-1
42	3	3
-3	1	0
-3	0	1

ELEMENT ACM

Approved for Public Release